

# Large-scale redistribution of maximum fisheries catch potential in the global ocean under climate change

WILLIAM W. L. CHEUNG\*<sup>†</sup>1, VICKY W. Y. LAM\*, JORGE L. SARMIENTO<sup>‡</sup>, KELLY KEARNEY<sup>‡</sup>, REG WATSON\*, DIRK ZELLER\* and DANIEL PAULY\*

\*Sea Around Us project, Fisheries Centre, 2202 Main Mall, Aquatic Ecosystems Research Laboratory, The University of British Columbia, Vancouver, British Columbia, Canada V5R 1E6, <sup>†</sup>School of Environmental Sciences, University of East Anglia, Norwich, NR4 7TJ, UK, <sup>‡</sup>Atmospheric and Oceanic Sciences Program, Princeton University, Sayre Hall, Forrestal Campus, PO Box CN710, Princeton, NJ 08544-7010, USA

## Abstract

Previous projection of climate change impacts on global food supply focuses solely on production from terrestrial biomes, ignoring the large contribution of animal protein from marine capture fisheries. Here, we project changes in global catch potential for 1066 species of exploited marine fish and invertebrates from 2005 to 2055 under climate change scenarios. We show that climate change may lead to large-scale redistribution of global catch potential, with an average of 30–70% increase in high-latitude regions and a drop of up to 40% in the tropics. Moreover, maximum catch potential declines considerably in the southward margins of semienclosed seas while it increases in poleward tips of continental shelf margins. Such changes are most apparent in the Pacific Ocean. Among the 20 most important fishing Exclusive Economic Zone (EEZ) regions in terms of their total landings, EEZ regions with the highest increase in catch potential by 2055 include Norway, Greenland, the United States (Alaska) and Russia (Asia). On the contrary, EEZ regions with the biggest loss in maximum catch potential include Indonesia, the United States (excluding Alaska and Hawaii), Chile and China. Many highly impacted regions, particularly those in the tropics, are socioeconomically vulnerable to these changes. Thus, our results indicate the need to develop adaptation policy that could minimize climate change impacts through fisheries. The study also provides information that may be useful to evaluate fisheries management options under climate change.

*Keywords:* catch, climate change, fisheries, global, marine, redistribution

*Received 21 December 2008; revised version received 13 April 2009 and accepted 6 May 2009*

## Introduction

Climate change is likely to affect the goods and services provided by ecosystems and its impacts on provisioning services such as food supply will have direct implication for the welfare of human society (e.g., Antle *et al.*, 2001; Easterling *et al.*, 2007; Battisti & Naylor, 2009). In terrestrial systems, using empirical and simulation modelling, food-crop production is projected to be negatively affected under the more intensive CO<sub>2</sub> emission scenarios, with most severe impacts projected for low-latitude

regions (e.g., Parry *et al.*, 2004, 2005; Fishcher *et al.*, 2005; Easterling *et al.*, 2007). Similar projections for pastures and livestock production have also been made (Easterling *et al.*, 2007). Although such projections are uncertain, they allow analysis of potential socioeconomic vulnerability, impacts on global food security and benefits and costs of climate change. In the marine biome, projections of climate change impacts on fisheries focus largely on a few species, regional climate variability and regime shifts, or qualitative inferences of potential changes (e.g., Lehodey, 2001; Lehodey *et al.*, 2003; Roessig *et al.*, 2004; Drinkwater, 2005; Brander, 2007). Despite the large contribution of marine capture fisheries to global animal protein supply [Pauly *et al.*, 2002; Food and Agriculture Organization (FAO), 2008], a global-scale projections of climate change impacts on marine fisheries is lacking.

Correspondence: William W. L. Cheung, tel. + 44 1603 593647, fax + 44 1603 591327, e-mail: William.cheung@uea.ac.uk

<sup>1</sup>Present address: School of Environmental Sciences, University of East Anglia, Norwich, NR4 7TJ, UK.

Marine fisheries productivity is likely to be affected by the alteration of ocean conditions including water temperature, ocean currents and coastal upwelling, as a result of climate change (e.g., Bakun, 1990; IPCC, 2007; Diaz & Rosenberg, 2008). Such changes in ocean conditions affect primary productivity, species distribution, community and foodweb structure that have direct and indirect impacts on distribution and productivity of marine organisms. Empirical and theoretical studies show that marine fish and invertebrates tend to shift their distributions according to the changing climate in a direction that is generally towards higher latitude and deeper water, with observed and projected rates of range shift of around 30–130 km decade<sup>-1</sup> towards the pole and 3.5 m decade<sup>-1</sup> to deeper waters (e.g., Perry *et al.*, 2005; Cheung *et al.*, 2008b, 2009; Dulvy *et al.*, 2008; Mueter & Litzow, 2008). Relative abundance of species within assemblages may also change because of the alteration of habitat quality by climate (e.g., Przeslawski *et al.*, 2008; Wilson *et al.*, 2008). Global primary production is projected to increase by 0.7–8.1% by 2050, with very large regional differences such as decreases in productivity in the North Pacific, the Southern Ocean and around the Antarctic continent and increases in the North Atlantic regions (Sarmiento *et al.*, 2004). Cheung *et al.* (2008a) has developed an empirical model that predicts maximum catch potential based on primary production and distribution range of 1066 species of exploited fishes and invertebrates. Such a model can be applied to evaluate how changes in primary productivity and species distributions under climate change would potentially affect fisheries productivity. Given the availability of projected primary productivity (Sarmiento *et al.*, 2004) and future distributions of major exploited marine fishes and invertebrates under climate change scenarios (Cheung *et al.*, 2009), it is possible to make quantitative projections of climate change impacts on global fisheries productivity.

Despite the uncertainty of global-scale projection of climate change impacts on fisheries productivity, such projection is useful in informing policy makers and stakeholders about the potential scale of the impact and in developing policy scenarios. Uncertainty exists in the prediction of primary productivity (Sarmiento *et al.*, 2004). Simultaneously, previous applications of bioclimate envelope models to project changes in species' distribution range have mixed success and failure. For example, predictions from selected bioclimate envelope models for bird species agree reasonably well with observations (e.g., Araújo *et al.*, 2005), while Beale *et al.* (2008), using null models developed from simulated distributions without climate association, reports that only 32 of 100 studied European bird species distributions show significant association with climate

variables. For marine ectotherms such as fish and shellfish, theoretical and empirical studies show that physiology, life history, productivity and distributions are strongly dependent on ocean conditions such as temperature (e.g., Pauly, 1980, 1981; Perry *et al.*, 2005; Dulvy *et al.*, 2008; Pörtner & Farrell, 2008; Pörtner *et al.*, 2008). However, the performance of models that project the effect of changes in ocean conditions on distributions and productivity of marine species has not been systematically assessed. Notwithstanding such uncertainty, projection of future distributions under changing ocean conditions is important, at least, in formulating null hypotheses of potential climate change impacts on marine species and fisheries (Cheung *et al.*, 2009).

In this study, we aim to project future changes in maximum catch potential from global oceans by 2055 under various climate change scenarios. Maximum catch potential is defined as the maximum exploitable catch of a species assuming that geographic range and selectivity of fisheries remain unchanged from the current (year 2005) level. We include 1066 species of marine fish and invertebrates, representing the major commercially exploited species, as reported in the FAO fisheries statistics (see <http://www.fao.org>), belonging to a wide range of taxonomic groups from around the world. Future distributions of these species are projected using a dynamic bioclimate envelope model (Cheung *et al.*, 2008b, 2009) while primary production is projected by empirical models (Behrenfeld & Falkowski, 1997; Carr, 2002; Marra *et al.*, 2003; Sarmiento *et al.*, 2004). Coupling these data with an empirical model (Cheung *et al.*, 2008a) allows us to project future changes in catch potential. The results should contribute to comprehensive assessments of climate change impacts on global socioeconomic and food security issues.

## Materials and methods

### *Projection of distributions of exploited fish and invertebrates*

Our analysis included 1066 species of exploited marine fishes and invertebrates, representing a wide range of taxonomic groups, ranging from krill, shrimps, anchovy and cod to tuna and sharks (see supporting information Table S3). Overall, they contributed 70% of the total reported global fisheries landings from 2000 to 2004 (*Sea Around Us* Project database: <http://www.seaaroundus.org>). The remaining 30% of the global landings was reported in the original FAO fisheries statistics as taxonomically aggregated groups such as groupers (Epinephelidae) and snappers (Lutjanidae). Because the

species composition of these aggregated groups is unknown, we did not include these groups in our analysis.

The distribution map of each species in recent decades (i.e., 1980–2000) was derived from an algorithm described in Close *et al.* (2006). Basically, this algorithm estimates the relative abundance of a species on a 30' latitude  $\times$  30' longitude grid of the world ocean. Input parameters for the model include the species' maximum and minimum depth limits, northern and southern latitudinal range limits, an index of association with major habitat types and known occurrence boundaries. The parameter values of each species, which could be retrieved from the *Sea Around Us* Project website (<http://www.seaaroundus.org/distribution/search.aspx>), were obtained from online databases such as FishBase (<http://www.fishbase.org>) and SealifeBase (<http://www.sealifebase.org>). Specifically, the index of habitat association scales from 0 to 1 (0: no association; 1: very strong association) and is a semiquantitative representation of the strength of association with specific habitats (see Cheung *et al.*, [http://www.seaaroundus.org/doc/saup\\_manual.htm](http://www.seaaroundus.org/doc/saup_manual.htm), for details of this index). The types of habitat include coral reef, seamounts, estuaries, inshore, offshore, continental shelf, continental slope and the abyssal. For all the 1066 species, we determined the index values from qualitative description of the species' biology and ecology. Based on the input parameters and predetermined rules on the latitudinal, bathymetric and habitat gradients of relative abundance, the model predicted a distribution map for each species (Close *et al.*, 2006). Thus, the model assumes that species distributions are directly or indirectly dependent on these factors.

We simulated future changes in species distribution by using a dynamic bioclimate envelope model (Cheung *et al.*, 2008b, 2009). First, the model identified species' preference profiles with environmental conditions that were defined by seawater temperature (bottom and surface), salinity, distance from sea-ice and habitat types (coral reef, estuaries, seamounts, coastal upwelling and a category that include all other habitat types). Regions of coastal upwelling were identified from temperature anomalies (see supporting information). Preference profiles are defined as the suitability of each of these environmental conditions to each species. Suitability, represented by the relative density of the species in each environmental conditions and habitat types, was calculated by overlaying environmental data (from 1980 to 2000) with maps of relative abundance of the species. For example, for each species, the model calculated a temperature preference profile based on the relative density of the species in different seawater temperature (Cheung *et al.*, 2009) (See Supplementary Information). Sea surface and bottom temperature data

were used for pelagic and demersal species, respectively.

Species' environmental preferences were linked to the expected carrying capacity in a population dynamic model in which growth, mortality and spatial dynamics of adult movement and larval dispersal along ocean currents were explicitly represented (Cheung *et al.*, 2008b, 2009). The model simulated changes in relative abundance of a species by

$$\frac{dA_i}{dt} = \sum_{j=1}^N G_i + L_{ji} + I_{ji} \quad (1)$$

where  $A_i$  is the relative abundance of a 30'  $\times$  30' cell  $i$ ,  $G$  is the intrinsic population growth and  $L_{ji}$  and  $I_{ji}$  are settled larvae and net migrated adults from surrounding cells, respectively.

Intrinsic growth is modelled by a logistic equation:

$$G_i = rA_i \left( 1 - \frac{A_i}{KC_i} \right) \quad (2)$$

where  $r$  is the intrinsic rate of population increase,  $A_i$  and  $KC_i$  are the relative abundance and population carrying capacity at cell  $i$ , respectively. The model assumes that carrying capacity varies positively with habitat suitability of each spatial cell and habitat suitability is dependent on the species' preference profiles to the environmental conditions (e.g., temperature, ice-coverage) in each cell. The final value of carrying capacity of a cell is calculated from the product of the habitat suitability of all the environmental conditions considered in the model. The model explicitly represents larval dispersal through ocean current with an advection–diffusion–reaction model (Cheung *et al.*, 2008b, 2009). The distance and direction of larval dispersal are a function of the predicted pelagic larval duration estimated based on an empirical equation (O'Connor *et al.*, 2007). In addition, animals are assumed to migrate along the calculated gradient of habitat suitability. Thus, changes in habitat suitability in each cell, determined by ocean conditions, lead to changes in the species' carrying capacity, population growth, net migration, and thus, relative abundance in each cell. Given the projected changes in ocean conditions and advection fields from ocean–atmosphere-coupled global circulation model (GCM) under climate change scenarios, the model simulated the annual changes in distribution of relative abundance of each species on the global 30'  $\times$  30' grid.

We included two climate scenarios, each representing high- and low-range greenhouse gas emissions. These included the Special Report on Emission Scenarios (SRES) A1B (CO<sub>2</sub> concentration at 720 ppm in 2100) and the stable-2000 level scenario (CO<sub>2</sub> concentration

maintains at year 2000 level of 365 ppm), respectively. Climate projections were generated by the Geophysical Fluid Dynamics Laboratory of the US National Oceanic and Atmospheric Administration (GFDL's CM 2.1; Delworth *et al.*, 2006). The original resolution of the outputs from the coupled model is 1° at latitudes higher than 30° north and south, with the meridional resolution becoming progressively finer towards the equator. We interpolated the physical variables from the coupled model with resolution of 30' in latitude and longitude using the Inverse Distance Weighted method, thus we avoided making complicated assumptions about the relationship between the coarser-resolution model outputs and their downscaled values.

#### *Projection of future primary production*

Using published empirical models and algorithms, we predicted primary production from the world ocean. First, to predict surface chlorophyll content in the ocean from GCM outputs, we used an empirical model described in Sarmiento *et al.* (2004). The model was developed by fitting chlorophyll data from SeaWiFS remote sensing to sea surface temperature, sea surface salinity, maximum winter mixed layer depth and length of growing season. Second, we used three published algorithms to predict ocean primary production. These algorithms, described in Carr (2002), Marra *et al.* (2003) and Behrenfeld & Falkowski (1997), calculate phytoplankton primary productivity as a function of the modelled surface chlorophyll content and its distribution, light supply and vertical attenuation, and sea surface temperature (Sarmiento *et al.*, 2004). All the physical parameters are outputs of the NOAA/GFDL's coupled model. The estimated annual average primary productivity is scaled onto a 30' latitude × 30' longitude grid. Thus, we predicted annual primary production in the world ocean from 2001 to 2060 for the two climate change scenarios using each of the above algorithms.

#### *Estimation of maximum catch potential*

Using a published empirical model described in Cheung *et al.* (2008a), we calculated the annual maximum catch potential for each of the spatial cells. The empirical model estimates a species' maximum catch potential (*MSY*) based on the total primary production within its exploitable range (*P*), the area of its geographic range (*A*), its trophic level ( $\lambda$ ) and includes terms correcting the biases from the observed catch potential (*CT*: number of years of exploitation and

*HTC*: catch reported as higher taxonomic level aggregations):

$$\log_{10}MSY_t = -2.991 + 0.826 \times \log_{10}P_t - 0.505 \times \log_{10}A_t - 0.152 \times \lambda + 1.887 \times \log_{10}CT + 0.112 \times \log_{10}HTC + \varepsilon \quad (3)$$

where *t* is year and  $\varepsilon$  is the error term. We assume that the proportion of exploitable range relative to the geographic range of a species ( $\alpha$ ) remains constant in the future. Thus, *P* was calculated from the sum of primary production (estimated from each of the three primary production algorithms) from the exploitable range weighted by the relative abundance (*Abd*) in each spatial cell (*i*):

$$P_t = \sum_{i=1}^n P'_{i,t} \alpha \frac{Abd_{i,t}}{MAX(Abd_{i,t})} \quad (4)$$

Range area (*A*) was the sum of area of all spatial cells that contribute to 95% of the total abundance (*n*) at year *t* from which distributions of relative abundance were simulated from the dynamic bioclimate envelope model described above. Trophic level ( $\lambda$ ) of each species was obtained from FishBase (<http://www.fishbase.org>), SeaLifeBase (<http://www.sealifebase.org>) and the *Sea Around Us* Project database (<http://www.seararoundus.org>) and was assumed to be constant over time. However, change in species distributions and community structure resulting from climate change may affect the trophic level of the species. This would affect the estimated change in maximum catch potential and remains a major uncertainty of our projections. The spatial distribution of the calculated maximum catch potential was assumed to be proportional to the relative abundance of each species in each cell.

We projected the global pattern of change in maximum catch potential from 2005 to 2055 under the two climate change scenarios. First, we calculated the predicted total maximum catch potential in each spatial cell for the 1066 species for each year from 2001 to 2060. To reduce the effect of interannual variability of the climate projections, we applied a 10-year running average to the estimated catch potential. We then plotted the percent change in catch potential in the world ocean between 2005 (i.e., average of 2001 to 2010) and 2055 (i.e., average of 2051 to 2060), with the ensemble mean of catch potential estimated from the three primary production algorithms. We also calculated the zonal (latitudinal) changes in total maximum catch potential of the period for each ocean basins and for the continental shelf ( $\leq 200$  m in depth) and offshore regions ( $>200$  m in depth). Bathymetry data are based on mean depth from real topography by



30' × 30' cell. To evaluate projected climate change impacts at country level, we aggregated our results by country's claimed Exclusive Economic Zone (EEZ).

## Results

### *Global maps of maximum catch potential by 2055*

Overall, although the projected total global maximum catch potential varies by  $\pm 1\%$  between 2005 and 2055 (10-year averages), climate change may considerably alter the distribution of catch potential, particularly between tropical and high-latitude regions (Fig. 1). Specifically, impacts in the Indo-Pacific region appear to be most intense, with up to 50% decrease in 10-year averaged maximum catch potential by 2055 under a higher greenhouse gas emission scenario (SRES A1B) (Fig. 1a). Simultaneously, catch potential in semi-enclosed seas such as the Red Sea and the southern coast of the Mediterranean Sea suffer from a reduction in

catch potential. In fact, catch potential from many coastal regions appear to decline. In addition, maximum catch potential in the Antarctic region declines considerably. By contrast, catch potential in the higher latitudinal regions, particularly the offshore regions of the North Atlantic, the North Pacific, the Arctic and the northern edge of the Southern Ocean increased greatly by more than 50% from the 2005 level. However, the pattern of change in catch potential is less clear under a low greenhouse gas emission scenario (Fig. 1b).

Studying the map of the absolute change in 10-year averaged maximum catch potential from 2005 to 2055, the change in the bulk of the catch concentrates along the continental shelf (Fig. 2). The projected baseline (10-year average in 2005) maximum catch potential concentrates along the continental shelf, offshore islands and mid-oceanic ridges or seamounts (Fig. 2a). These also coincide with areas where large changes in catch potential occur. Particularly, we project a large reduction in catch potential in the tropics,

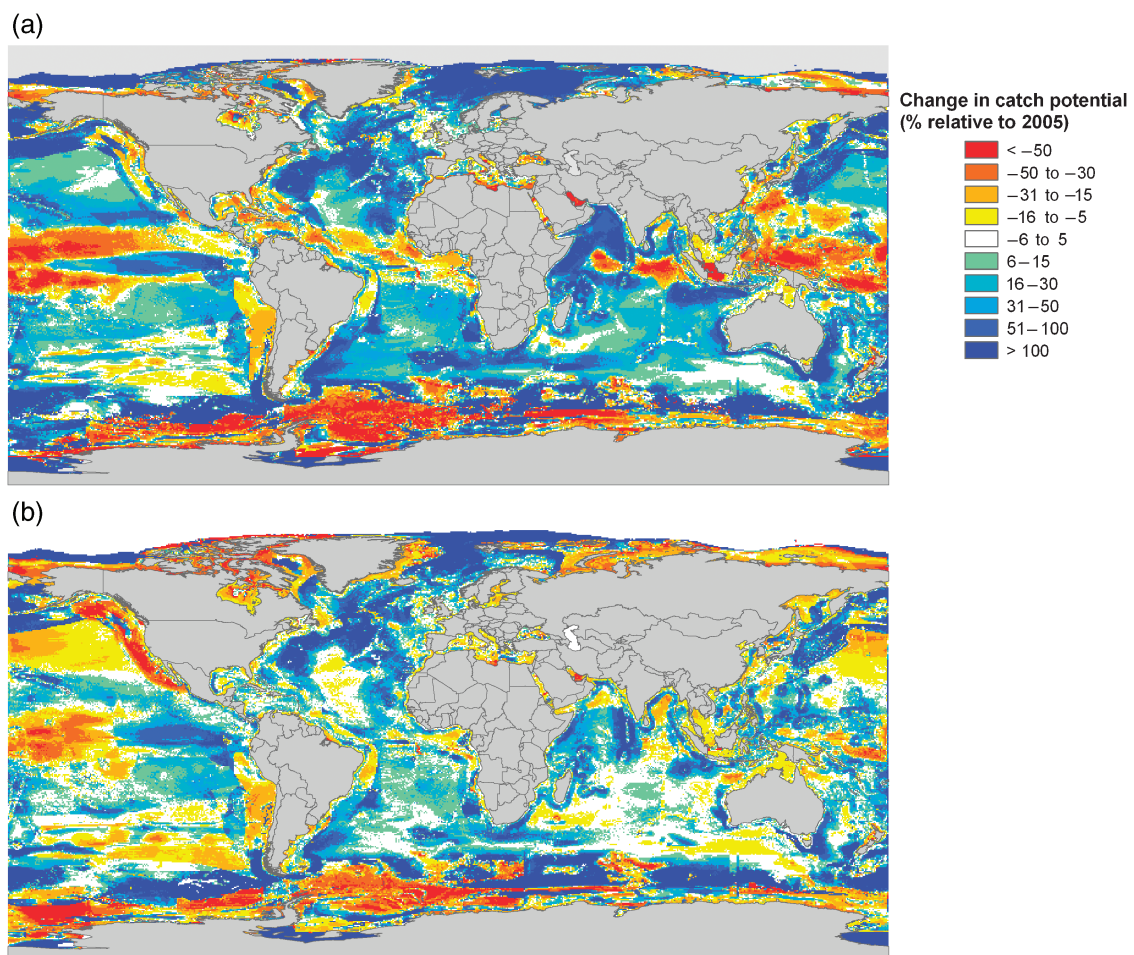


**Fig. 1** Change in maximum catch potential (10-year average) from 2005 to 2055 in each 30' × 30' cell under climate change scenarios: (a) Special Report on Emission Scenarios A1B and (b) stabilization at 2000 level.

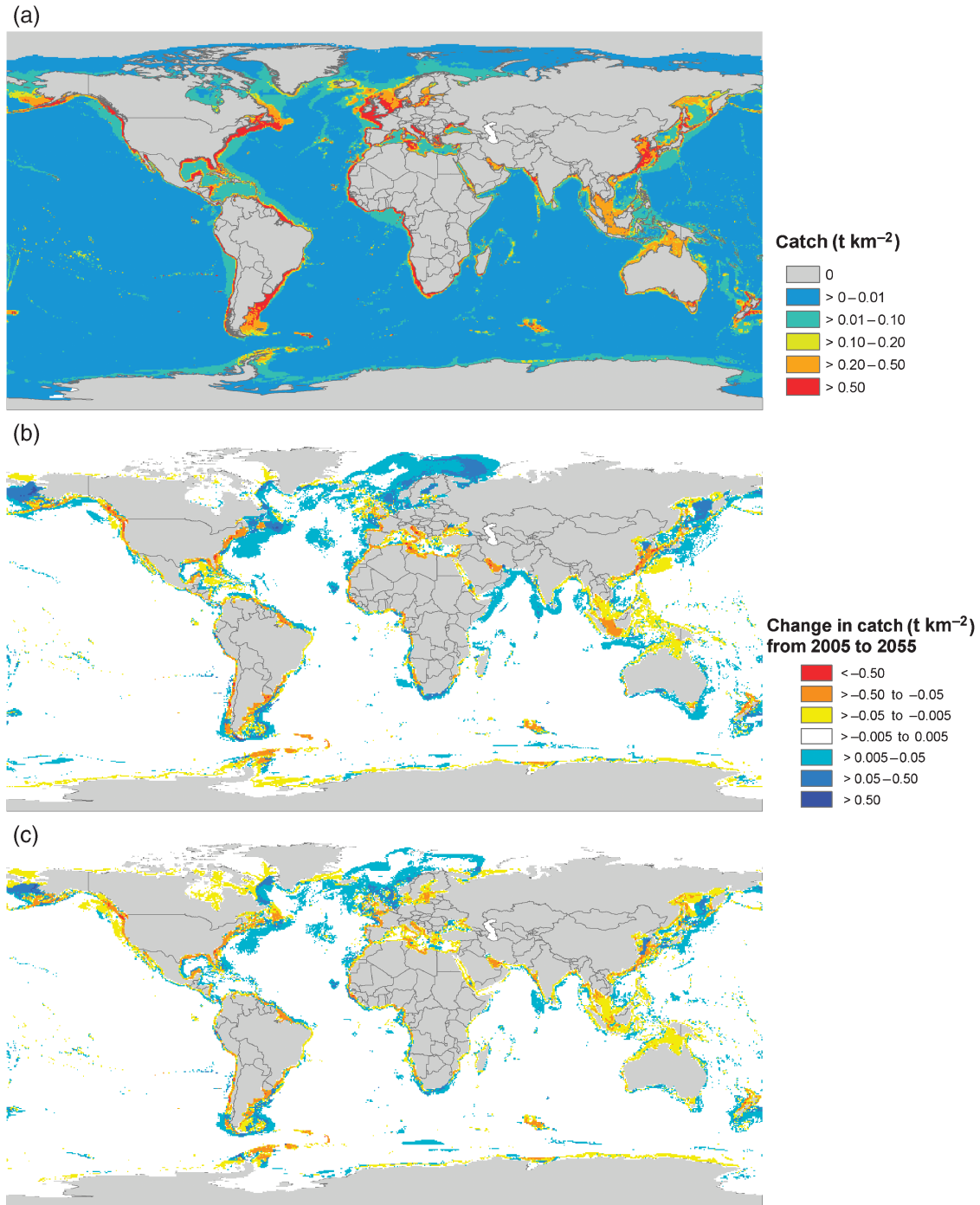


**Fig. 2** The estimated 10-year averaged maximum catch potential for 2005 (a) and the difference in the absolute catch potential between 2005 and 2055 under two climate change scenarios: (b) Special Report on Emission Scenarios A1B and (c) stabilization at 2000 level.

semienclosed seas and inshore waters, while catch potential increases largely in the North Atlantic, North Pacific (particularly the Bering Sea) and the poleward tips of continental margins such as around South Africa, southern coast of Argentina and Australia (Fig. 2b and c).

*Zonal average change in maximum catch potential*

The general pattern observed from the map can be better illustrated by the zonal-average changes in maximum catch potential (Fig. 3). Globally, 10-year average maximum catch potential reduces by up to 20% from

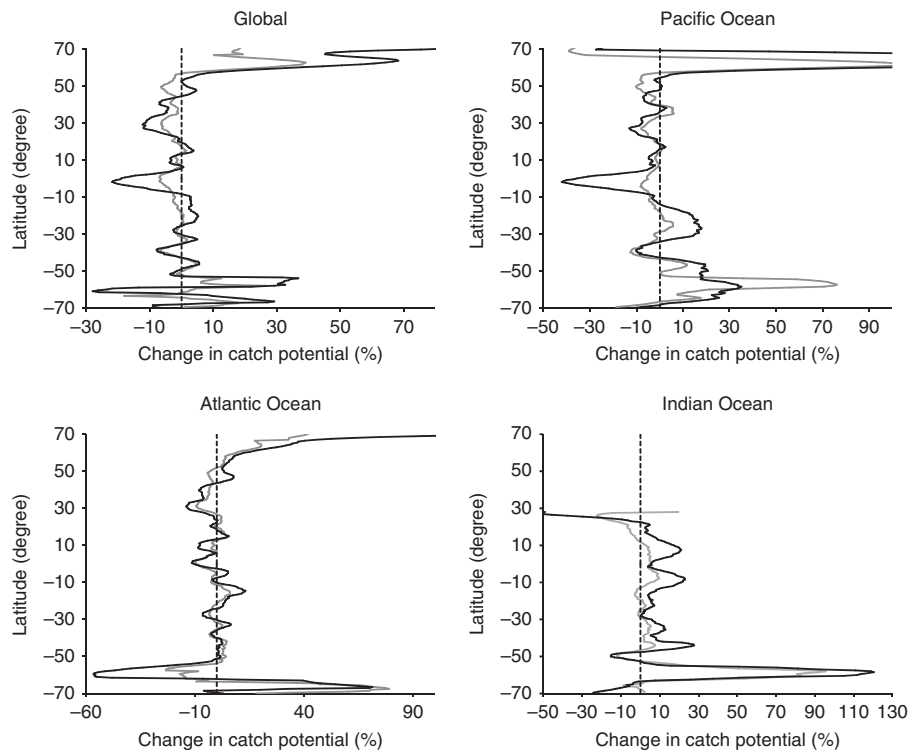


**Fig. 3** Projected zonal (latitudinal) changes in 10-year average maximum catch potential from 2005 to 2055 under the high-range (black line) and low-range (grey line) greenhouse gas emission scenarios. Resolution of the latitudinal zones was originally in 30', which was then smoothed by 5° latitude running averages to reduce the variability from the finer resolution. The dotted line indicates no change in catch potential.

2005 to 2055 in areas between 10°N and 10°S under the high-range greenhouse gas emission scenario (Fig. 3a). In the northern hemisphere, catch potential declines moderately in the temperate regions (around 25°–50°N) but increases in the higher latitudinal regions, particularly the subarctic. In the southern hemisphere, the pattern is less clear in nontropical regions, except that there are large variations in changes in maximum catch potential ( $\pm 30\%$  from 2005 level) around the Antarctic region. Overall, under the low-range greenhouse gas emission scenario, projected changes in catch potential show a similar pattern, but with lower magnitudes of changes.

The zonal pattern of change varies in different ocean basins. In the Pacific Ocean, the pattern of change in 10-year average maximum catch potential parallels the global trend, but with a much higher magnitude of change (Fig. 3b). For example, catch potential in the tropical Pacific is projected to decrease by up to 42% from the 2005 level, while those in the sub-Arctic region doubled the 2005 level. In the Atlantic Ocean, the projected magnitudes of change in the tropical and temperate regions is much smaller than those in the global average and the Pacific Ocean (Fig. 3c), and

mostly within 10% of changes from the 2005 level. However, the projected large increase in catch potential around the poles is consistent with projections for the global ocean. In the Indian Ocean, the projected trend in the tropics is different from other ocean basins, with considerable increase in catch potential by up to 20% from the 2005 level under the high-range scenario (Fig. 3d). Moreover, catch potential declines largely along the northward continental boundary of the Indian Ocean.

The zonal average shows a clear contrast between the changes in 10-year average maximum catch potential in the continental shelf and offshore regions (Fig. 4). Under a high-range greenhouse gas emission scenario, projected catch potential from the continental shelf decreases throughout most of the latitudinal zones by 2055 except in the high-latitude region (Fig. 4a). In contrast, projected catch potential increases considerably in offshore regions, except around the equator (0°) where projected increase in catch potential is relatively low. Relative to the shelf-offshore pattern of change in catch potential, the variation in projected changes under the three different primary production estimation algorithms is small (Fig. 4b and c).

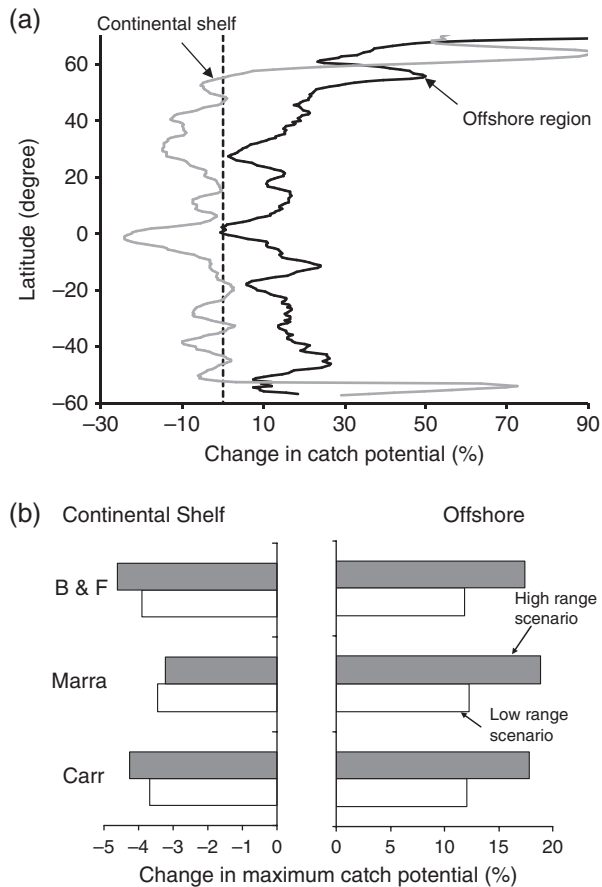


**Fig. 4** Projected changes in 10-year average maximum catch potential from 2005 to 2055 in continental shelf (depth  $\leq 200$  m, grey line) and offshore (depth  $> 200$  m, black line) regions: (a) zonal (latitudinal) averages under the high-range greenhouse gas emission scenarios. Bathymetry is based on mean depth from real topography by  $30' \times 30'$  cell. Resolution of the latitudinal zones was originally in  $30'$ , which was then smoothed by  $5^\circ$  latitude running averages to reduce the variability from the finer resolution. The dotted line indicates no change in catch potential. (b) Global changes of maximum catch potential in continental shelf and offshore regions in two climate change scenarios under the three primary production estimate algorithms (Carr – Carr, 2002; Marra – Marra *et al.*, 2003; B & F – Behrenfeld & Falkowski, 1997).

#### Changes in maximum catch potential by EEZ regions

Aggregating maximum catch potential by 240 EEZ regions (see <http://www.seaaroundus.org>), we find that some high-latitude countries/regions in the northern hemisphere largely gain in catch potential, while many tropical and subtropical countries/regions may lose (Fig. 5). Among the 20 Atlantic EEZ regions with the highest recorded catch in the 2000s, 10-year averaged catch potentials in Nordic countries/regions such as Norway, Greenland and Iceland are projected to

increase by 18–45% under the high-range emission scenario (SRES A1B). In the Pacific, catch potentials from Alaska and Russia are projected to increase by around 20%. On the other hand, catch potential from most other EEZ regions declined to varying degrees, with tropical and subtropical countries/regions such as Indonesia having the largest projected decline by 2055. The projected decline in catch potential in the United States (excluding Alaska and Hawaii), China, Chile and Brazil are moderate, ranging from 6% to 13% under the high-range emission scenario.

#### Comparison between greenhouse gas emission scenarios

Comparing between the high- and low-range (stabilization at 2000-level) scenarios, the average changes in catch potential by 2055 for all the 240 EEZ regions under the high-range scenario are generally 1.6 times the changes under the low-range scenario (Fig. 6). The relationship between the projections from the two climate change scenarios is described by a linear relationship with a slope of 1.6 and a zero intercept ( $P < 0.05$ ,  $r^2 = 0.58$ ). Thus, the projected climate change impact on catch potential in EEZ regions is positively related to the level of greenhouse gas emission.

#### Discussion

Our results suggest that climate change may have a large impact on the distribution of maximum catch potential – a proxy for potential fisheries productivity – by 2055. Such a redistribution of catch potential is driven by projected shifts in species' distribution ranges and by the change in total primary production within the species' exploited ranges (Sarmiento *et al.*, 2004; Cheung *et al.*, 2008a). In the tropics and the southern margin of semienclosed seas such as the Mediterranean Sea, species are projected to move away from these regions as the ocean warms up. Thus, the catch potential in these regions decreases considerably. Simultaneously, ocean warming and the retreat of sea ice in high-latitude regions opens up new habitat for lower-latitude species and thus may result in a net increase in catch potential. Moreover, catch potential increases in the poleward continental margins (e.g., southern parts of Australia and Africa) because most commercially exploited species are associated with continental shelves. Thus these continental margins represent a limit of species' distribution shifts. In subtropical and temperate regions, cold-water species are replaced by warm-water species, rendering the trend in catch potential changes in these regions generally weaker than in tropical, high-latitude and polar regions. The large reduction in catch potential in the southern ocean



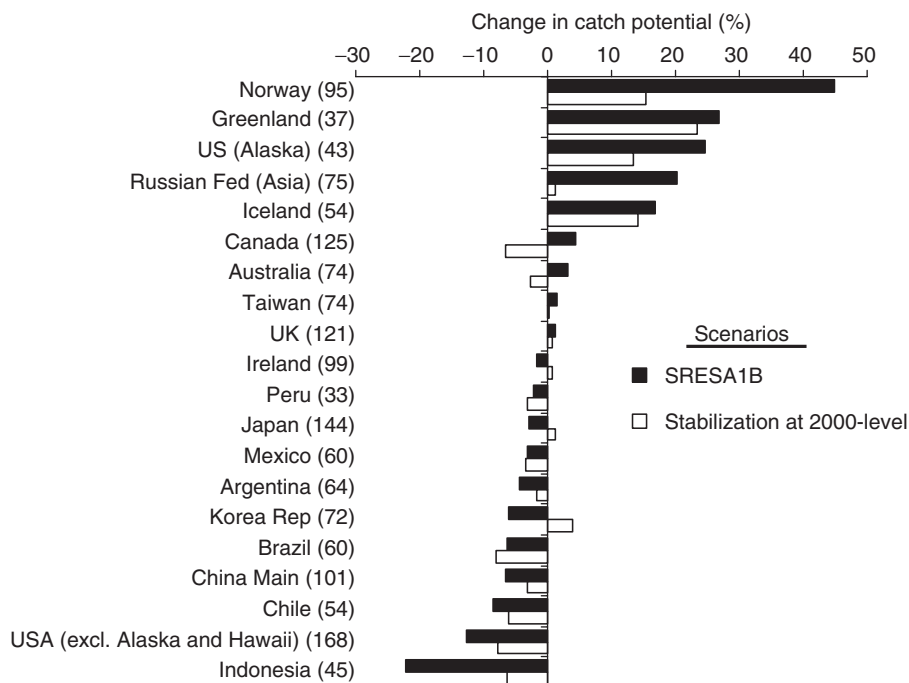


**Fig. 5** Projected changes in 10-year averaged maximum catch potential from 2005 to 2055 by the 20 Exclusive Economic Zone regions with the highest catch in the 2000s. The numbers in parentheses represent the numbers of exploited species included in the analysis.

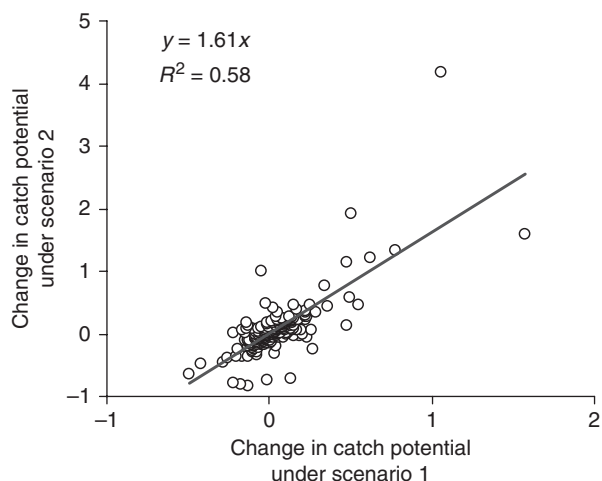


**Fig. 6** The projected change in 10-year averaged maximum catch potential from 2005 to 2055 between the high-range greenhouse gas emission scenario (Special Report on Emission Scenarios A1B, scenario 2) and the low-range scenario (Stabilization at 2000-level, scenario 1) for 240 Exclusive Economic Zone regions is roughly proportional, with the high-range scenario having approximately 1.6 times higher impact than the low-range scenario. The line was obtained from a linear regression of projections from the two scenario with intercept = 0. As the linkages between greenhouse gas concentration, ocean conditions and fisheries potential are complex, the high variability of the points from the fitted line is expected.

is the result of a shift in the lower-latitude range boundary of many Antarctic species, resulting in a loss of catch potential. In addition, as species move offshore to colder refuges as the ocean warms up, catch potential also shifts to offshore regions from coastal areas. Such inshore-to-offshore shifts as estimated here corroborate observations from field studies (Dulvy *et al.*, 2008).

The projected change in maximum catch potential may have large implications for global food security. If the decrease in catch potential in tropical countries is directly translatable to actual catches, climate change may have a negative impact on food security in many tropical communities that are strongly dependent on fisheries resources for food and revenues. Such communities may already have high socioeconomic vulnerability to climate change in fisheries (Allison *et al.*, 2009). In fact, the reduction in catch potential in tropical countries and the increase in high-latitude countries coincide with similar projections for terrestrial-based food production systems such as agriculture and livestock farming (Easterling *et al.*, 2007). Given that agricultural food production in many tropical developing countries may become vulnerable to climate change, the additional stress from the reduction in fisheries catch potential may further exacerbate the food security problem. The problem is especially apparent in the Pacific, where climate change is projected to have very different impacts between the tropical and high

latitudinal regions. The offshore shift of catch potential may also render fishing activities more costly as fishing boats may have to operate further offshore. In addition, as most marine fisheries resources in the world are currently fully exploited, over-exploited or collapsed and the global marine catch appears to reach or has exceeded its biological limits (Pauly *et al.*, 2002; FAO, 2008), it is expected that climate-induced changes in catch potential will strongly affect global fisheries production and food supply.

While this study provides an important basis to understand climate change impacts on marine capture fisheries, various uncertainties are associated with our projections. Firstly, we did not consider the effect of changes in eco-physiology, such as the increased physiological stress resulting from ocean acidification (e.g., Orr *et al.*, 2005; Pörtner & Farrell, 2008; Cheung *et al.*, 2009). These factors would likely have negative impacts on the maximum catch potential. Secondly, projections from dynamic bioclimate envelope model are uncertain (Cheung *et al.*, 2009). The current distribution maps may not adequately reflect species' habitat preferences. Accurate estimates of population and dispersal parameters were not available. However, sensitivity analysis of the dynamic bioclimate envelope model shows that its projections are generally robust to key input parameters (Cheung *et al.*, 2008b). Also, our projected rates of range-shift for exploited fishes are of similar magnitude to the observed rates in the North Sea (Perry *et al.*, 2005) and the Bering Sea (Mueter & Litzow, 2008) in recent decades (Cheung *et al.*, 2009; W. W. L. Cheung, unpublished data); this provides support to the validity of our projections. Distribution shifts may be influenced by species' evolutionary or physiological adaptation, and interactions between species or anthropogenic factors that were not captured in our model (Davis *et al.*, 1998; Harley *et al.*, 2006; Hsieh *et al.*, 2008). Consideration of these factors is expected to increase the rate of range-shifting of the species; thus our projected distribution shifts are considered conservative (Cheung *et al.*, 2009). Moreover, there are uncertainties associated with projections of ocean conditions that were applied to predict primary production and changes in species distributions. Particularly, because of the coarse resolution of the GCM, representation of dynamics in finer spatial resolution (e.g., coastal processes) is particularly uncertain. Also, we do not explicitly consider the responses of fisheries to potential changes in species distribution and catch potential. We implicitly assume that the exploitable area of a species follows the species distribution. However, the validity of this assumption is uncertain, depending on changes in fishing dynamics. Such changes depend on a network of factors, including changes in fishing costs and revenues, global and local

demand and supply of seafood and the global trade system. Based on the experience from studying climate change impacts on food supply from agriculture and livestock production systems, these socioeconomic factors are important in evaluating climate change impacts (e.g., Parry *et al.*, 2004, 2005; Easterling *et al.*, 2007). This study provides a basis for incorporating these factors for future analysis.

Our projected catch potential is less sensitive to the choice of particular algorithms for estimating primary production relative to the effects of the projected shifts in range areas (see supporting information Fig. S5). Because of the difference in predicted change in primary production at high temperature between models, the projected changes in primary production in the low-latitude regions vary. Specifically, the Behrenfeld & Falkowski (1997) method has a polynomial temperature-dependence function that predicts a decrease in primary productivity at higher temperature, whereas the Carr (2002) and Marra *et al.* (2003) methods have a more physiological-like temperature-dependence function that predicts exponential increase in primary productivity as temperature increases. As a result, using the Behrenfeld & Falkowski (1997) method, a decrease in primary production by 2055 was calculated, but an increase was calculated from the Carr (2002) and Marra *et al.* (2003) methods (Sarmiento *et al.*, 2004). However, most of the exploited marine species considered in this study have large distribution ranges. Their maximum catch potentials are estimated from integrating primary production from large areas, which dampens the effect of the variation in the change of primary production on the projected maximum catch potential. Thus, globally, projected change in maximum catch potential is not sensitivity to the different primary production estimation algorithms. Regionally, the tropical region (between 30° north and south) is relatively more sensitive to the different algorithms with the Behrenfeld and Falkowski algorithm predicts slightly stronger decrease in maximum catch potential than the predictions using the Carr and Marr algorithms (see supporting information). However, such differences do not affect the pattern of changes and the overall conclusion of the analysis. Moreover, we use an ensemble mean of projected catch potential projected from the different primary production algorithms, thus making our projected catch potential more robust to the uncertainty in primary production estimation.

## Conclusions

This study projects climate change impacts on global catch potential, which is a fundamental step towards filling the gap of predicting future food supply from the

ocean and the livelihood of people depending on marine fisheries resources. Our estimates suggest that the high-range greenhouse gas emission could result in a world-wide redistribution of maximum catch potential and the level of impacts is positively related to the emission level. Remaining conservative, we did not include the highest emission level scenario considered by the IPCC (e.g., SRES A1F), and it is expected that such a scenario would result in much stronger impacts on maximum catch potential.

### Acknowledgements

We thank A. Gelchu, S. Hodgson, A. Kitchingman and C. Close for their work on the *Sea Around Us* Project's species distribution ranges. We are grateful to the NOAA Geophysical Fluid Dynamics Laboratory for producing the climate projections. This is a contribution by the *Sea Around Us* Project, a scientific cooperation between the University of British Columbia and the Pew Charitable Trust, Philadelphia.

### References

- Allison E, Perry A, Badjeck M *et al.* (2009) Vulnerability of national economies to the impacts of climate change on fisheries. *Fish and Fisheries*, **10**, 173–196.
- Antle J, Apps M, Beamish R *et al.* (2001) Ecosystems and their goods and services. In: *Climate Change 2001: Impacts, Adaptation, and Vulnerability* (eds McCarthy JJ, Canziani OF, Leary NA *et al.*), pp. 237–340. Cambridge University Press, Cambridge.
- Araújo MB, Pearson RG, Thuiller W, Erhard M (2005) Validation of species-climate impact models under climate change. *Global Change Biology*, **11**, 1504–1513.
- Bakun A (1990) Global climate change and intensification of coastal ocean upwelling. *Science*, **247**, 198–201.
- Battisti D, Naylor RL (2009) Historical warnings of future food insecurity with unprecedented seasonal heat. *Science*, **323**, 240–244.
- Beale CM, Lennon JJ, Gimona A (2008) Opening the climate envelope reveals no macroscale associations with climate in European birds. *Proceedings of the National Academy of Sciences of the United States of America*, **105**, 14908–14912.
- Behrenfeld MJ, Falkowski PG (1997) A consumers guide to phytoplankton primary production models. *Limnology and Oceanography*, **42**, 1479–1491.
- Brander KM (2007) Global fish production and climate change. *Proceedings of the National Academy of Sciences of the United States of America*, **104**, 19709–19714.
- Carr ME (2002) Estimation of potential productivity in Eastern Boundary Currents using remote sensing. *Deep Sea Research Part II*, **49**, 59–80.
- Cheung WWL, Close C, Lam V *et al.* (2008a) Application of macroecological theory to predict effects of climate change on global fisheries potential. *Marine Ecology Progress Series*, **365**, 187–197.
- Cheung WWL, Lam VWY, Pauly D (2008b) Dynamic bioclimate envelope model to predict climate-induced changes in distribution of marine fishes and invertebrates. In: *Modelling Present and Climate-Shifted Distributions of Marine Fishes and Invertebrates. Fisheries Centre Research Reports 16(3)* (eds Cheung WWL, Lam VWY, Pauly D), pp. 5–50. University of British Columbia, Vancouver.
- Cheung WWL, Lam VWY, Sarmiento JL *et al.* (2009) Projecting global marine biodiversity impacts under climate change scenarios. *Fish and Fisheries*. doi: 10.1111/j.1467-2979.2008.00315.x.
- Close C, Cheung WWL, Hodgson S *et al.* (2006) Distribution ranges of commercial fishes and invertebrates. In: *Fishes in Databases and Ecosystems. Fisheries Centre Research Report 14(4)* (eds Palomares D, Stergiou KI, Pauly D), pp. 27–37. University of British Columbia, Vancouver.
- Davis AJ, Jenkinson LS, Lawton JH, Shorrocks B, Wood S (1998) Making mistakes when predicting shifts in species range in response to global warming. *Nature*, **391**, 783–786.
- Delworth TL, Rosati A, Stouffer RJ *et al.* (2006) GFDL's CM2 global coupled climate models. Part I: formulation and simulation characteristics. *Journal of Climate*, **19**, 643–674.
- Diaz RJ, Rosenberg R (2008) Spreading dead zones and consequences for marine ecosystems. *Science*, **321**, 926–929.
- Drinkwater KF (2005) The response of Atlantic cod (*Gadus morhua*) to future climate change. *ICES Journal of Marine Science*, **62**, 1327–1337.
- Dulvy NK, Rogers SI, Jennings S, Stelzenmüller V, Dye SR, Skjoldal HR (2008) Climate change and deepening of the North Sea fish assemblage: a biotic indicator of warming seas. *Journal of Applied Ecology*, **45**, 1029–1039.
- Easterling WE, Aggarwal PK, Batima P *et al.* (2007) Food, fibre and forest products. In: *Climate Change 2007: Impacts, Adaptation and Vulnerability* (eds Parry ML, Canziani OF, Palutikof JP *et al.*), pp. 273–313. Cambridge University Press, Cambridge.
- Food and Agriculture Organization (FAO) (2008) *The State of World Fisheries and Aquaculture (SOFIA)*. FAO, Rome.
- Fishcher G, Shah M, Tubiello FN *et al.* (2005) Integrated assessment of global crop production. *Philosophical Transactions of the Royal Society of London: B*, **360**, 2067–2083.
- Harley C, Huges DG, Hultgren AR *et al.* (2006) The impacts of climate change in coastal marine systems. *Ecology letters*, **9**, 453–460.
- Hsieh C, Reiss CS, Hewitt RP *et al.* (2008) Spatial analysis shows that fishing enhances the climate sensitivity of marine fishes. *Canadian Journal of Fisheries and Aquatic Sciences*, **65**, 947–961.
- IPCC (2007) Summary for policymakers. In: *Climate Change 2007: The Physical Science Basis. Working Group I Contribution to the Fourth Assessment Report of the IPCC* (eds Solomon S, Qin D, Manning M *et al.*), pp. 1–18. Cambridge University Press, Cambridge.
- Lehodey P (2001) The pelagic ecosystem of the tropical Pacific Ocean: dynamic spatial modelling and biological consequences of ENSO. *Progress in Oceanography*, **49**, 439–468.
- Lehodey P, Chai F, Hampton J (2003) Modelling climate-related variability of tuna populations from a coupled ocean-biogeochemical populations dynamics model. *Fisheries Oceanography*, **12**, 483–494.

- Marra J, Ho C, Trees CC (2003) *An Algorithm for the Calculation of Primary Productivity from Remote Sensing Data*. Lamont-Doherty Earth Obs., Palisades, NY.
- Mueter FJ, Litzow MA (2008) Sea ice retreat alters the biogeography of the Bering Sea continental shelf. *Ecological Applications*, **18**, 309–320.
- O'Connor MI, Bruno JE, Gaines SD *et al.* (2007) Temperature control of larval dispersal and the implications for marine ecology, evolution and conservation. *Proceedings of the National Academy of Sciences of United States of America*, **104**, 1266–1271.
- Orr JC, Fabry VJ, Aumont O *et al.* (2005) Anthropogenic ocean acidification over the twenty-first century and its impact on calcifying organisms. *Nature*, **437**, 681–686.
- Parry M, Rosenzweig C, Livermore M (2005) Climate change, global food supply and risk of hunger. *Philosophical Transactions of the Royal Society of London: B*, **360**, 2125–2138.
- Parry ML, Rosenzweig C, Lglesias A *et al.* (2004) Effects of climate change on global food production under SRES emissions and socio-economic scenarios. *Global Environmental Change*, **14**, 53–67.
- Pauly D (1980) On the interrelationships between natural mortality, growth parameters and mean environmental temperature in 175 fish stocks. *Journal du Conseil International pour l'Exploration de la Mer*, **39**, 175–192.
- Pauly D (1981) The relationships between gill surface area and growth performance in fish: a generalization of von Bertalanffy's theory of growth. *Berichte der Deutschen Wissenschaftlichen-Kommission für Meeresforschung*, **28**, 251–282.
- Pauly D, Christensen V, Guénette S *et al.* (2002) Towards sustainability in world fisheries. *Nature*, **418**, 689–695.
- Perry AL, Low PJ, Ellis JR *et al.* (2005) Climate change and distribution shifts in marine fishes. *Science*, **308**, 1912–1915.
- Pörtner HO, Bock C, Knust R *et al.* (2008) Cod and climate in a latitudinal cline: physiological analyses of climate effects in marine fishes. *Climate Research*, **37**, 253–270.
- Pörtner HO, Farrell AP (2008) Physiology and climate change. *Science*, **322**, 690–692.
- Przeslawski R, Ah Yong S, Byrne M *et al.* (2008) Beyond corals and fish: the effects of climate change on noncoral benthic invertebrates of tropical reefs. *Global Change Biology*, **14**, 2773–2795.
- Roessig JM, Woodley CM, Cech JJ (2004) Effects of global climate change on marine and estuarine fishes and fisheries. *Reviews in Fish Biology and Fisheries*, **14**, 251–275.
- Sarmiento JL, Slater R, Barber R *et al.* (2004) Response of ocean ecosystems to climate warming. *Global Biogeochemical Cycles*, **18**, GB3003 doi: 10.1029/2003GB002134.
- Wilson SK, Fisher R, Pratchett MS *et al.* (2008) Exploitation and habitat degradation as agents of change within coral reef fish communities. *Global Change Biology*, **14**, 2796–2809.

## Supporting Information

Additional Supporting Information may be found in the online version of this article:

**Figure S1.** Brief summary of the structure of the dynamic bioclimate envelope model developed in this study which was implemented in Visual Basic.Net environment.

**Figure S2.** Distribution of relative abundance (A) and the inferred temperature preference profile (TPP) (B) of the Small yellow croaker (*Larimichthys polyactis*).

**Figure S3.** A series of cells at the same latitude within the same ocean basin. *T* is the sea surface temperature at each particular cell.

**Figure S4.** Map showing the upwelling indexes assigned to each upwelling region.

**Figure S5.** Projected zonal (latitudinal) change in 10 years average maximum catch potential calculated between 2005 and 2055 using the three primary production estimation algorithms: B & F – Behrenfeld & Falkowski, 1997; Marra – Marra *et al.*, 2003; Carr – Carr, 2002. Globally, projected change in maximum catch potential is not sensitivity to the different primary production estimation algorithms (A, top). Regionally, the tropical region (between 30° north and south) is relatively more sensitivity to the different algorithms (B, bottom) with the B & F algorithm predicts slightly stronger decrease in maximum catch potential than the predictions using the Carr and Marr algorithms. However, the selection of particular algorithm does not affect the overall conclusion of the analysis.

**Table S1.** List of environmental and species distribution variables and the sources of data that the dynamic bioclimate envelope model accounts for in predicting the current and future distributions of marine fish and invertebrate.

**Table S2.** Upwelling index computed from the SST anomalies data or wind-induced upwelling data. Regions with upwelling index equal to 6 have the strongest upwelling. Regions would have the weakest upwelling within the upwelling region if their index value is 1.

**Table S3.** List of families of the 1066 species of marine fish and invertebrates that are included in the analysis.

Please note: Wiley-Blackwell are not responsible for the content or functionality of any supporting materials supplied by the authors. Any queries (other than missing material) should be directed to the corresponding author for the article.